In-situ Construction of TiO_2/Ag Heterojunction Coating for Forming a Photocatalytic Self-cleaning Surface of Concrete

Jun Feng[1,2], Kai Zhang[3], Shuyou Huang, Jie Zhang[2] , Bowen Huo[2], Xishu Cao[2], Peijiang Cong[*,2]

[1] Department of Materials and Science Engineering, Dalian Jiaotong University, Dalian, Liaoning Province, 116028, China

[2] College of Water Conservancy and Environmental Engineering, Changchun Institute of Technology, Changchun, Jilin Province, 130012, China

[3] Research Center of Earthquake Engineering, China Institute of Water Resources and Hydropower Research, Beijing 100048, China

[*] Corresponding author: Peijiang Cong

E-mail: congpeijiang@126.com, tel: 0431-80578567

Graphical abstract

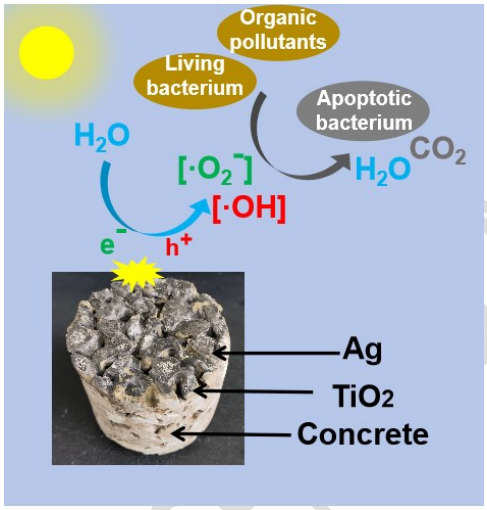

Abstract

As a widely used construction material, concrete is an ideal substrate for environmental functional materials. However, ordinary concrete lacks pollution resistance. When exposed to the natural environment, it is easily susceptible to microbial growth or organic contamination. Therefore, it is necessary to enhance its surface cleaning ability through modification methods. The existing anti-pollution materials are cumbersome to prepare and have a short lifespan. In this study, we employed in-situ synthesis to construct a TiO_2/Ag coating on the surface of concrete. When illuminated, the catalyst coating generates electron-hole pairs, and with the synergistic acceleration of the heterojunction interface and oxygen defects, they separate and react with water to produce hydroxyl radicals and superoxide radicals. Under simulated sunlight with an intensity of 50mW/cm^2, this material can achieve an 86.4% organic matter decomposition rate and a 96.7% microbial inactivation rate, and

it can remain stable over ten cycles. This study presents a viable technical solution for the design of sustainable self-cleaning building materials.
Keywords： anti-pollution, concrete, TiO_2/Ag, photocatalysis, coating

1. introduction

Sponge city is an environmentally friendly urban construction concept (Qiao et al., 2020), which can minimize the impact of urban development on the ecological environment by absorbing and utilizing natural precipitation through buildings. In this process, porous pervious concrete is widely used in the construction of sponge cities (Qi et al., 2023). However, concrete materials exposed to nature are easily contaminated by rainwater erosion, air dust and other environmental pollution, which can accumulate pollutants on the surface (Jiang et al., 2016) and breed microorganisms (Kiledal et al., 2021). As dirt and biofilm grow, they will erode the basic structure of concrete and reduce its lifespan. On the other hand, this surface pollution is not only unsightly, but also poses a potential threat to human health, indicating the need to clean contaminated concrete building materials (Nath et al., 2016). However, the cost of periodic manual cleaning of concrete surface pollutants is too high, which requires the development of self-cleaning concrete materials (Topçu et al., 2020).

Photocatalysis is a green and sustainable chemical technology (Rammohan et al., 2013), which uses photocatalysts excited by natural light to effectively decompose pollutants and deactivate attached microorganisms. It is an ideal direction for developing self-cleaning concrete. In previous studies, researchers have enhanced the pollution resistance of concrete by incorporating pollution-resistant nanomaterials (Guo et al., 2020), but this method requires excessive nanomaterial consumption, making it impractical in terms of cost. Other researchers have developed environmentally friendly coatings containing nanomaterials (Petronella et al., 2018), which not only have higher catalyst concentrations compared to doping technology, but also reduce usage costs. However, this approach still faces the problem of the active surface area of nanomaterials being obscured by other components of the coating (Abbas et al., 2020), leading to decreased activity. In addition, the stability of the applied coating is poor and easily peels off under natural conditions (Zhang et al., 2022). Therefore, there is a need to develop a simple and efficient coating method based on existing materials, while simultaneously considering the catalyst loading concentration and stability (Munafo et al., 2015).

In this study, we used a coating-burning method to construct TiO_2/Ag coatings on the surface of concrete in situ, completely wrapping the concrete surface with anti-pollution nanomaterials, greatly increasing the catalyst loading. At the same time, the coating-burning method not only allows for scaling up production through spraying equipment or rapid on-site preparation, but also benefits from high-temperature sintering, tightly bonding the coating to the concrete, eliminating the possibility of paint peeling. Through simulated pollutant decomposition experiments, microbial inhibition experiments, and corresponding cyclic tests, the developed method in this study has been proven to have good photocatalytic self-cleaning performance. The catalytic mechanism of the material was explored through

characterization techniques such as X-ray photoelectron spectroscopy, laser confocal microscopy, and electron paramagnetic resonance. The main catalytic mechanism is the accelerated carrier transfer effect of the coupled TiO_2-Ag heterojunction interface and oxygen defect, promoting the generation of hydroxyl radicals and superoxide radicals, ultimately achieving self-cleaning based on free radical oxidation.

2. Experiment

2.1. Materials and reagents

Pervious precast porous concrete blocks with a strength of C25 or greater were purchased to be used as the concrete substrate required for this study. (https://b2b.baidu.com/, SR04, Jiangsu Hainiu New Material Co., China).

Tetrabutyl titanate, silver nitrate, anhydrous ethanol, sodium chloride, and methylene blue were used as the chemicals required for the preparation of coatings and experiments in this experiment. The purity of the above reagents are all analytically pure, and they were purchased from Sinopharm Chemical Reagent Co. Ultrapure water (resistivity ≥18.2 MΩ-cm) was used for the preparation and dilution of the reagents used in the experiments.

2.2. Preparation of modified concrete

5 mL of ethanol containing 10 % by volume of tetrabutyl titanate was dropped onto the surface of a cylindrical concrete sample with a top diameter of 6 cm (approximately 28.3 cm^2 in area). Dried in a 60 ℃ oven, repeated this process three times. Then the sample was heated in a muffle furnace at 400 ℃ for 10 hours to obtain the concrete/TiO_2 sample.

5 mL of 100 g/L silver nitrate aqueous solution was dropped evenly onto the top of the concrete/TiO_2 sample, dried in a 60 ℃ oven, then the sample was heated in a muffle furnace at 400 ℃ for 4 hours to obtain the concrete/TiO_2/Ag sample.

2.3. Culture and Enumeration of Microorganisms

Escherichia coli (ATCC25922) was used as the indicator bacterium in this study. Before each experiment, the frozen bacterial suspension stored in the -80 ℃ freezer needs to be activated for two generations in liquid LB medium. The main steps are as follows: the bacterial strain is taken out from the frozen storage tube and thawed in a water bath. Then, 0.5 mL of the bacterial solution is inoculated into liquid LB medium and cultured at 37 ℃ for 20 hours. After that, 1 mL of the first generation activated bacterial solution is re-inoculated into a new liquid LB medium and cultured at 37 ℃ for 10 hours. Finally, the activated bacterial solution is centrifuged at 4 ℃ and 4500 $r*min^{-1}$ for 10 minutes, the supernatant is removed, and the bacteria are resuspended with physiological saline as a bacterial stock solution.

The plate counting method was used to detect the total number of Escherichia coli colonies in the samples. After thoroughly mixing the samples, gradient dilution is performed, and 1 mL of the water sample is used to prepare the agar plates using the pour plate method. After culturing at 37 ℃ for 20 hours, the colony total number in the sample is determined.。

2.4. Experimental Methods

Photocatalytic decomposition of methylene blue experiment: under the light of a xenon lamp at 50 mW/cm^2, the prepared concrete columns were added to 100 mL of an aqueous solution containing 100 μg/L methylene blue, and 3 mL of samples were taken every half hour for 2 hours. The dark adsorption experiment was not necessary because the inclusion of a blank control group and a catalyst-free column concrete experimental group was able to reflect factors other than catalytic decomposition that led to the reduction of methylene blue concentration (mainly concrete adsorption).

Photocatalytic antimicrobial experiments: the prepared concrete columns were added to 100 mL of an aqueous solution containing 10^5 CFU/mL of E. coli under the illumination of a xenon lamp at 50 mW/cm^2, and 3 mL of samples were taken every half an hour for 2 hours. Special attention should be paid to the fact that the top of the beaker needs to be covered with a 1 mm thick transparent organic plastic sheet in order to avoid the trace amount of short-wave UV contained in the xenon lamp from affecting the antimicrobial simulation experiments. In addition, dark adsorption experiments were likewise replaced by more representative blank control and concrete experiments.

Laser confocal microscopy staining experiments: 5 μmol/L SYTO-9 was used to stain live bacteria into green fluorescence, 2 μg/mL PI solution was used to stain apoptotic bacteria into red fluorescence, 500 μL of staining solution was gently dripped on the surface of the samples, and the samples were stained for 15 minutes at 37 ℃ under irradiation protection, and then washed off the staining solution gently with physiological saline, which is the stained samples ready for photographing on the machine.

2.5. Characterisation of samples

The concentration of methylene blue was measured by the colourimetric method using an ultraviolet spectrophotometer (SHIMADZU, UV1800). Scanning electron microscopy (SEM), energy dispersive spectroscopy (EDS), X-ray diffraction spectroscopy (XRD), X-ray photoelectron spectroscopy (XPS), and electron paramagnetic resonance (EPR) results were provided by the third-party testing organisation, Biotest (https://www.zkbaice.cn/). Confocal Laser Scanning Microscopy (CLSM) was provided by the third-party testing organisation Science Compass (https://www.shiyanjia.com/). The specific instrument model and related parameters can be obtained at the above web site for more details. In addition, due to the hardness of the concrete samples, the samples were mainly obtained by cracking and flattening the samples, and only the XPS tests were obtained by scraping the powder.

3. Results and discussions

3.1. Heterogeneous junction coating morphology on concrete surfaces

Through the macroscopic real-shot images of the sample and the microscopic surface images under the scanning electron microscope, it can be preliminarily judged whether the material in this study has the expected good morphology. As shown in Figure 1a, in this study, a coating of titanium dioxide and elemental silver was constructed layer by layer on the surface of columnar concrete blocks through the impregnation-burning method, and named as concrete, concrete/TiO_2 and concrete/TiO_2/Ag. Among them, the concrete is mainly gray, and its untreated surface

has a relatively flat microscopic morphology (Figure 1b), composed of hundreds of nanometer-sized concrete strips (Figure 1e). The upper surface of the columnar concrete loaded with titanium dioxide obviously turns white, which is the macroscopic manifestation of a large amount of titanium dioxide nanoparticles being loaded. Correspondingly, in Figure 2c, it can be clearly seen that large particles of titanium dioxide grow on the surface of the concrete, and studies have shown that these sharp edges can directly cause physical damage to microorganisms (Liu et al., 2021), inhibiting biological activity. Finally, with the loading of the silver coating, the upper surface changes from white to black, which is the macroscopic manifestation of a large amount of nano-silver being loaded. These nano-silver particles are much smaller than the large particles of titanium dioxide (Figure 1d). Comparing the relatively smooth surface of concrete/TiO_2 (Figure 1d) and the relatively rough surface of concrete/TiO_2/Ag (Figure 1g), it can be seen that the nano-silver is uniformly sized 50nm spherical nanoparticles, which tightly cover the surface of the titanium dioxide, forming a double-layer heterogeneous structure. Therefore, it can be confirmed that the synthesized samples in this study have the expected obvious layered loading structure.

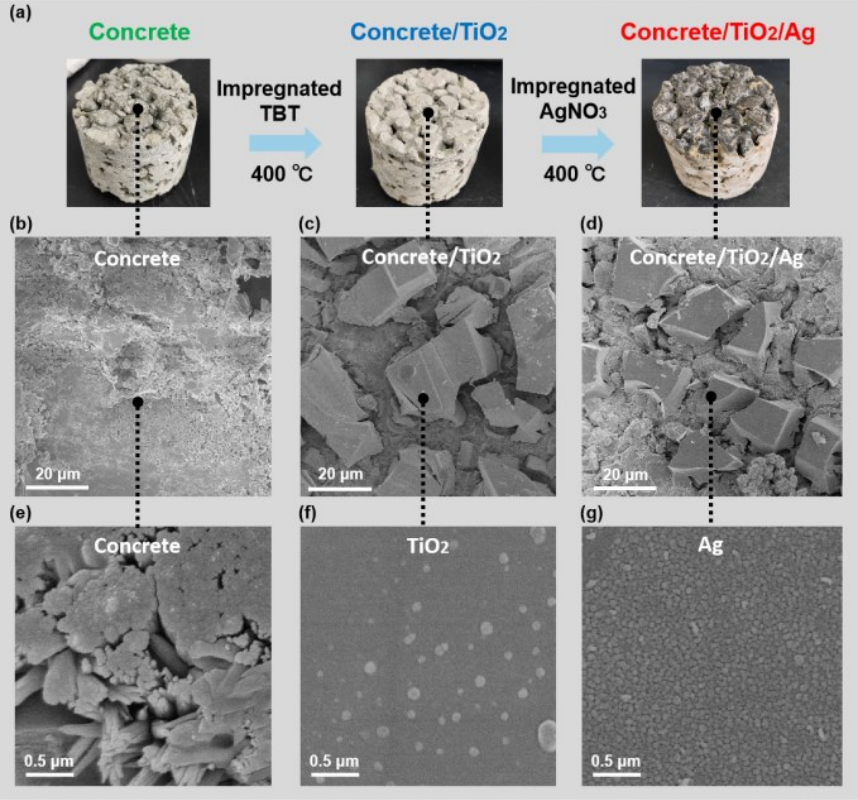

Figure 1. (a) Actual morphology of the samples of concrete, concrete/TiO_2 and concrete/TiO_2/Ag with the synthesis flow chart. (b) SEM images of concrete, (c) concrete/TiO_2 and (d) concrete/TiO_2/Ag. (e) Local magnification SEM images of concrete, (f) concrete/TiO_2 and (g) concrete/TiO_2/Ag.

3.2. Analysis of elemental content and distribution

By analyzing the energy spectrum test of scanning electron microscopy, the element content of the material can be analyzed. The surface-selected area element distribution

test of concrete samples (Figure 2a-a6) shows that the atomic weight of the main elements in the concrete selected in this study is in descending order of oxygen, carbon, calcium, silicon, and aluminum (Figure 2b). Carbon mainly comes from calcium carbonate and surface organic pollutants, while silicon and aluminum mainly come from aluminosilicate. Trace amounts of titanium may be derived from natural minerals containing small amounts of titanium ore. These natural mineral impurities have high impurity content and poor crystallinity. They basically do not have photocatalytic activity, so they often only appear as carriers in catalytic reactions (Zhao et al., 2019), rather than catalysts.

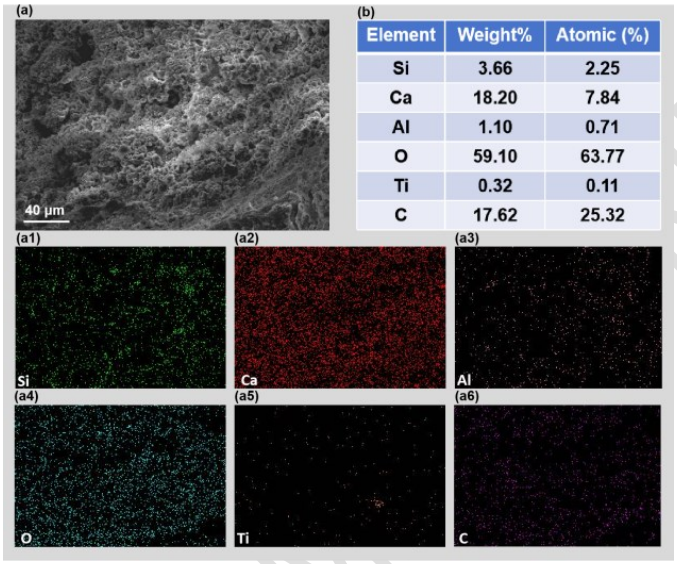

Figure 2. concrete of the elemental distribution images of the selected area with (a) SEM image and (b) elemental content, and distribution images of each element: (a1) Si, (a2) Ca, (a3) Al, (a4) O, (a5) Ti, and (a6) C.

In the elemental distribution map of the concrete/TiO_2/Ag sample (Figure 3a), it can be clearly seen that the bright spots of silicon (Figure 3a1) and aluminum (Figure 3a3) have a similar distribution, but differ from the distribution of calcium. This confirms the previous speculation that the substance is composed of calcium carbonate and silicate, and the two are not uniformly mixed. On the other hand, the oxygen (Figure 3a4) and titanium (Figure 3a5) elements overlap highly, and are highly exclusive with the calcium element, which strongly proves the loading of TiO_2 particles on the surface of concrete. Interestingly, the silver element (Figure 3a6) not only overlaps with the titanium element, but also coincides with the calcium element. This indicates that the silver element covers both the TiO_2 particles and the surface of the concrete in the gaps, which can prevent the growth of microorganisms in the gaps between the catalyst particles.

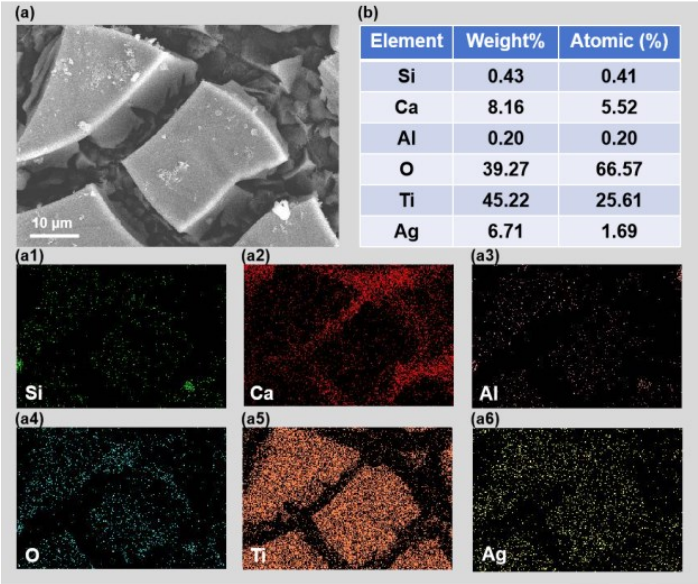

Figure 3. elemental distribution images of concrete/TiO_2/Ag (a) SEM image and (b) elemental content of the selected area, and distribution images of each element: (a1) Si, (a2) Ca, (a3) Al, (a4) O, (a5) Ti, (a6) Ag.

3.3. Analysis of the chemical properties of crystals

After analyzing the sample morphology using electron microscopy, further investigation of the connection between concrete and catalyst coatings was conducted through X-ray diffraction and X-ray photoelectron spectroscopy. In the comparison of XRD patterns for the three samples (Figure 4a), the green peak representing concrete in the range of 20° to 30° was not distinctly evident in concrete/TiO_2. However, the blue peaks at around 25.3° and 48° were attributed to the (101) and (200) crystal planes of rutile-phase titanium dioxide (PDF#78-2486), indicating that the titanium dioxide coating effectively covered the concrete surface with good crystallinity. This also explains the masking of crystal peaks in concrete. Furthermore, with the loading of elemental silver, multiple distinct peaks attributed to elemental silver (PDF#04-0783) were observed, along with weaker characteristic peaks of titanium dioxide, indicating the formation of crystalline metallic silver on the surface of titanium dioxide. In the overall XPS spectrum (Figure 4b), compared to the results for concrete/TiO_2, an increase in the Ag3d peak was observed in concrete/TiO_2/Ag, further confirming the formation of a heterogeneous structure between silver and titanium dioxide. In the Ti2p XPS spectrum, it was found that the binding energy of titanium in concrete/TiO_2/Ag shifted to higher values compared to that in concrete/TiO_2, reflecting the loss of electrons by the titanium element (Shang et al., 2021). This phenomenon indicates electron transfer from titanium dioxide to silver nanoparticles at the TiO_2-Ag heterogeneous interface. These results demonstrate the close association between large titanium dioxide particles and silver nanoparticles, as well as the presence of interface charge carrier migration, which is conducive to the separation and transfer of photogenerated electron-hole pairs under light excitation, thereby possessing enhanced photocatalytic activity.

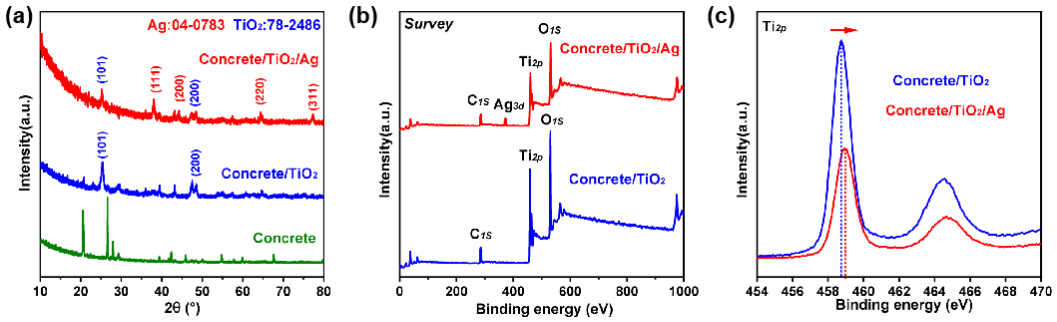

Figure 4. (a) XRD patterns of concrete, concrete/TiO_2 and concrete/TiO_2/Ag. comparison of XPS (b) full and (c) titanium spectra of concrete/TiO_2 and concrete/TiO_2/Ag.

3.4. Comparison of photocatalytic anti-pollution performance

To validate the exceptional photocatalytic performance of the developed concrete/TiO_2/Ag in this study, experiments were conducted to simulate the organic decomposition and antibacterial properties of modified concrete materials through photocatalytic degradation of methylene blue and deactivation of Escherichia coli, evaluating its photocatalytic self-cleaning ability. In Figure 5a, the black line shows that simulated sunlight hardly induces methylene blue decomposition within 3 hours, while the green line indicates that concrete can remove some methylene blue, possibly due to the adsorption effect of the concrete material (Abetua et al., 2021). The better removal effect shown by the blue line indicates that the titanium dioxide loaded on the concrete surface can effectively photocatalytically decompose methylene blue. The red line demonstrates the optimal removal effect, indicating that elemental silver significantly enhances the photocatalytic activity of concrete/TiO_2/Ag. The stability of the photocatalytic activity of concrete/TiO_2/Ag was confirmed in cyclic experiments. In Figure 5b, it is evident that concrete/TiO_2/Ag maintained an 80% degradation rate after ten cycles of use, whereas conversely, the concentration of methylene blue in the solution of the unmodified concrete remained stable at a level similar to photodegradation after four uses, indicating that its adsorption effect on methylene blue reached saturation and lacked persistent anti-pollution capability.

The materials developed in this study not only showed promising photocatalytic decomposition of organic matter, but also inactivated disease-causing microorganisms. In Figure 5c, the black line indicates that light exposure only slightly deactivated Escherichia coli in the solution, and with the addition of concrete, the green line shows a significant downward trend, possibly related to the adsorption effect of the concrete. The blue line of the concrete/TiO_2 sample exhibits a lower residual bacterial concentration, indicating the photocatalytic antibacterial effect of titanium dioxide on the concrete surface. Similar to Figure 5a, the red line reaches the lowest point, indicating the strongest inhibitory effect of concrete/TiO_2/Ag on Escherichia coli under light exposure. Furthermore, in cyclic experiments, it is observed that concrete/TiO_2/Ag can maintain stable antibacterial capability over ten consecutive long-term uses, whereas unmodified concrete, after effectively adsorbing Escherichia coli twice, shows a noticeable decrease in adsorption capability. Starting from the

sixth use, the concrete instead leads to an increase in the concentration of Escherichia coli in the solution, possibly related to the formation of bacterial biofilm (Gaylarde et al., 1999), which can block the pore structure on the surface of concrete blocks and protect the bacteria in the solution from harmful substances in the concrete. Therefore, unmodified concrete, apart from its brief adsorption capability, lacks the ability to resist pollutant contamination and may even provide a platform for microbial growth, necessitating the construction of a TiO_2/Ag coating on its surface to achieve self-cleaning ability under light exposure.

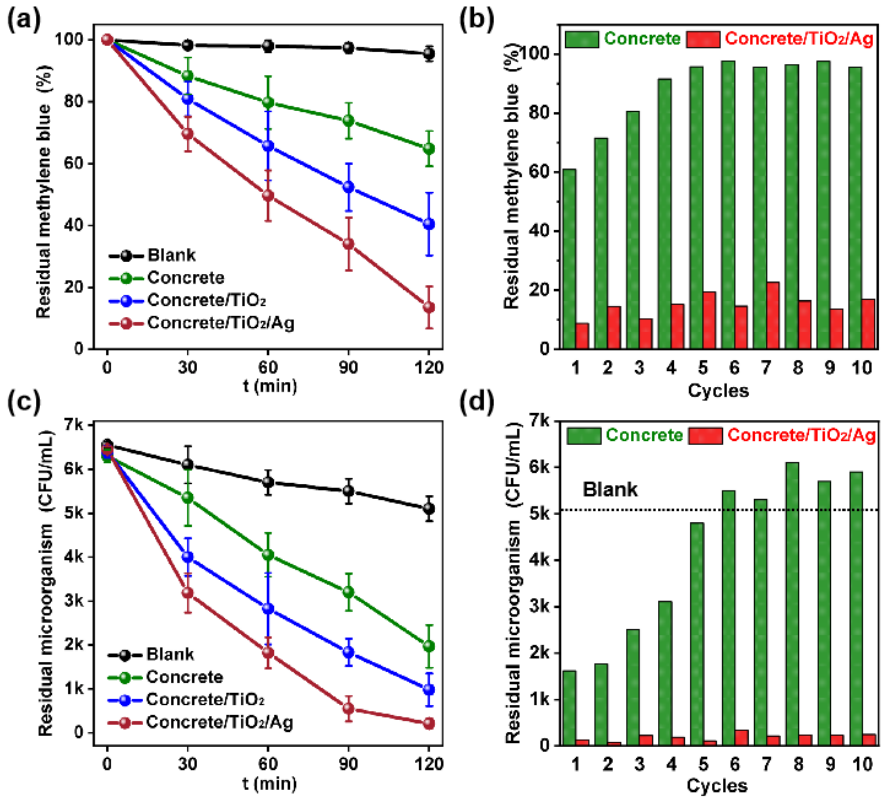

Figure 5. (a) A comparison of the performance of the photodegradation of methylene blue in the blank control group with only light exposure, unmodified concrete, and modified concrete. (b) The photocatalytic degradation effect of methylene blue in unmodified concrete and modified concrete during ten cycles of use. (c) A comparison of the performance of the photocatalytic inactivation of Escherichia coli in the blank control group with only light exposure, unmodified concrete, and modified concrete. (d) The photocatalytic inactivation effect of Escherichia coli in unmodified concrete and modified concrete during ten cycles of use.

3.5. Evaluation of resistance to biological contamination

To investigate the self-cleaning ability of modified concrete more intuitively, a laser confocal microscope was used to observe the survival of E. coli on the material surface after a two-hour light exposure antibacterial experiment. In Figure 6, green fluorescence represents live bacteria, and red fluorescence represents dead bacteria. Obviously, a large number of bacteria survived on the surface of the concrete (Figure 6a), which is not conducive to the long-term use of the material. In contrast, the concrete/TiO_2 sample loaded with titanium dioxide coating showed a certain degree of

reduction in green fluorescence (Figure 6b), indicating its certain photocatalytic antibacterial performance. Excitingly, the green fluorescence on the surface of the concrete/TiO_2/Ag sample is almost invisible (Figure 6c), indicating that the loading of TiO_2/Ag heterojunction greatly enhances the antibacterial ability of the material. No red fluorescence was observed in Figure 6d, indicating that there were no dead bacteria on the surface of the concrete, which also confirms our speculation: the removal of E. coli from water by concrete under light exposure (Figure 5d) mainly comes from adsorption rather than inactivation. In contrast, some dead bacteria appeared on the surface of concrete/TiO_2 (Figure 6e), indicating that titanium dioxide can inactivate some microorganisms through catalysis under light exposure. In stark contrast, the surface of concrete/TiO_2/Ag showed a very strong red fluorescence response (Figure 6f). Combined with the weak green fluorescence in Figure 6c, we can conclude that almost all microorganisms attached to the surface of concrete/TiO_2/Ag have been inactivated under light exposure, which strongly proves that the heterojunction coating developed in this study can effectively resist microbial contamination of concrete with the help of light excitation (Gladis et al., 2010).

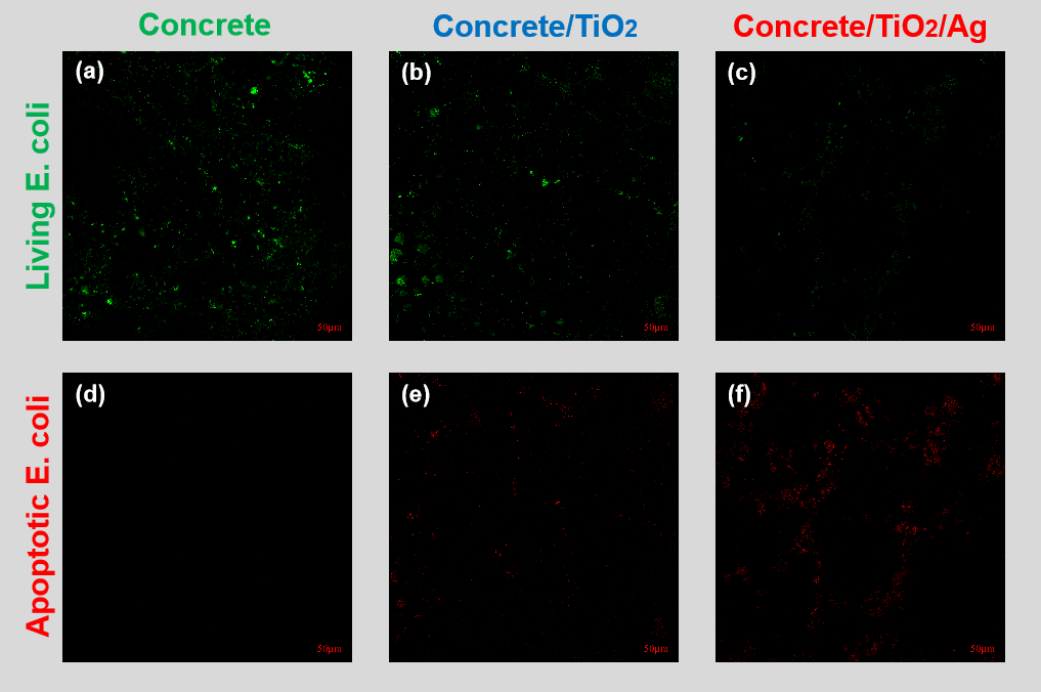

Figure 6. fluorescence imaging of living bacteria under laser confocal microscopy for (a) concrete, (b) concrete/TiO_2 and (c) concrete/TiO_2/Ag. (d) Fluorescence imaging of apoptotic bacteria under laser confocal microscopy of (d) concrete, (e) concrete/TiO_2 and (f) concrete/TiO_2/Ag.

3.6. Generation of photocatalytically active species

After comparing the pollution resistance of modified and unmodified concrete interfaces, the self-cleaning mechanism of TiO_2/Ag on the concrete surface was investigated using electron paramagnetic resonance (EPR) technique. From figures 6a and 6b, it is evident that the concrete itself does not generate free radicals under light excitation. However, concrete/TiO_2 modified with titanium dioxide can simultaneously generate hydroxyl radicals and superoxide radicals. Furthermore,

concrete/TiO_2/Ag further enhances the generation of these two types of free radicals. These photo-catalytically generated reactive oxygen species effectively decompose organic compounds and eradicate microorganisms (Cho et al., 2004). The accelerated generation of these active species is attributed to the separation of photo-generated electron-hole pairs by the TiO_2/Ag heterojunction structure and the accelerated mass transfer at various active sites on the interface. The detection of oxygen vacancy concentration in the material provides strong evidence for this viewpoint, as shown in figure 7c. The concrete surface does not contain oxygen vacancies, while concrete/TiO_2 contains a certain amount of oxygen vacancies. The oxygen vacancy concentration is further enhanced in concrete/TiO_2/Ag, and oxygen vacancies act as defect-bound excitons, extending the lifetime of photo-generated electrons and serving as active sites to accelerate interfacial mass transfer (Huang et al., 2022). Studies have indicated that lattice oxygen defects carry positive charges, which enhance the formation of free radicals at the interface (Khiem et al., 2024). This is consistent with the phenomenon of increased generation of positively charged holes in figure 7d as titanium dioxide and elemental silver are sequentially loaded onto the concrete surface. It is worth noting that the detection of holes is achieved using TEMPO, which is a persistent free radical and exhibits a strong signal in EPR tests. The holes generated by light excitation in the material will quench the signal of TEMPO, so a lower signal represents a higher hole generation. Consequently, the photo-generated holes in concrete/TiO_2/Ag are significantly higher than in concrete/TiO_2. The dual-layer TiO_2/Ag heterostructure coating exhibits a significantly higher generation of free radicals and a more pronounced effect of electron-hole separation compared to the single-layer titanium dioxide coating, demonstrating stronger photocatalytic activity.

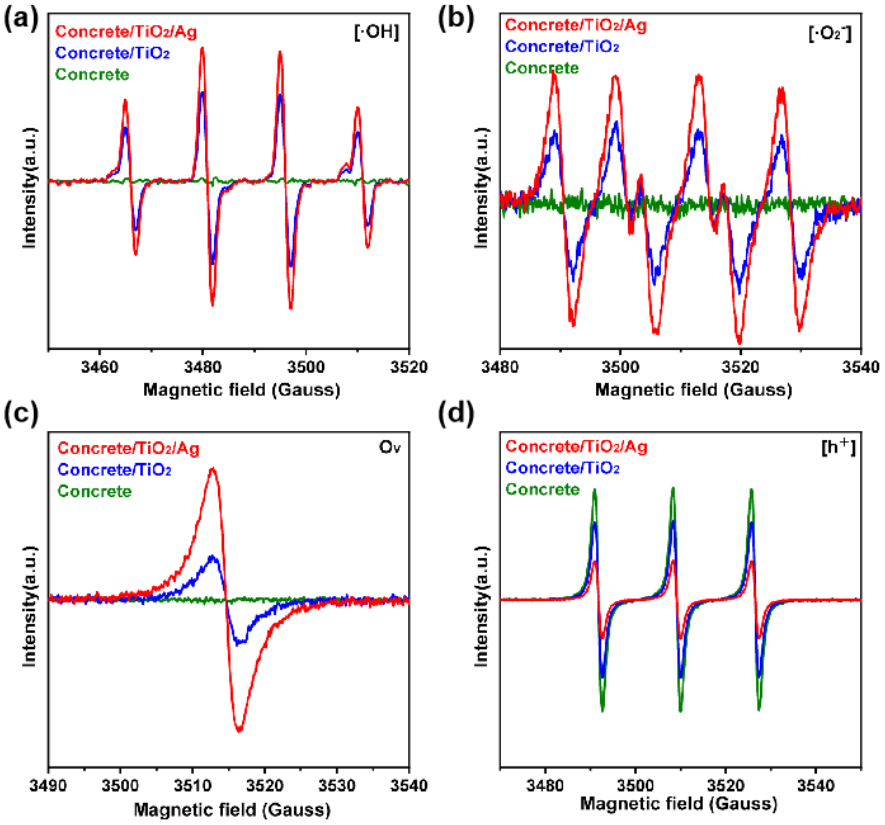

Figure 7. (a) Amount of photogenerated hydroxyl radicals, (b) amount of photogenerated superoxide radicals, (c) concentration of oxygen vacancies, and (d) amount of photogenerated holes of concrete, concrete/TiO_2, and concrete/TiO_2/Ag obtained by EPR testing.

3.7. Photocatalytic self-cleaning mechanism for modified concrete

Based on the preceding results, a schematic diagram of the photocatalytic self-cleaning mechanism of the developed material in this study is summarized. As shown in Figure 8, under light excitation, the titanium dioxide coating on the concrete surface absorbs photons, generating electron-hole pairs in the excited state. The electrons undergo interfacial mass transfer and inject into the silver nanoparticles (Figure 4c), while the holes accumulate on the surface of the titanium dioxide, achieving effective electron-hole separation. The electrons and holes on the coating surface react with water to produce superoxide radicals and hydroxyl radicals, which decompose organic pollutants in water into carbon dioxide and water. Simultaneously, they oxidize and deactivate live bacteria into apoptotic bacteria, thereby achieving the photocatalytic self-cleaning of concrete.

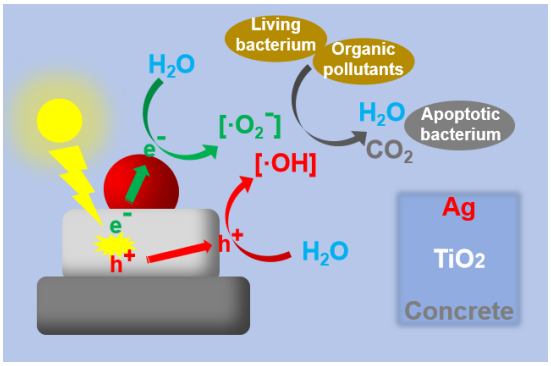

Figure 8. photocatalytic self-cleaning mechanism of concrete/TiO_2/Ag.

4. conclusion

In summary, this study developed a method to construct TiO_2/Ag heterojunction coating on the surface of concrete in situ, creating an environmentally functional material with good self-cleaning properties under light. Tests including SEM-EDS, XRD, and XPS confirmed that the well-shaped TiO_2/Ag heterojunction coating stably adhered to the concrete surface, with effective interaction between titanium dioxide and silver monomer. EPR tests showed that the material can generate a large number of photo-generated electrons and holes under light excitation, converting them into superoxide radicals and hydroxyl radicals, effectively decomposing organic compounds and deactivating bacteria, with the help of the electron-hole separation effect of the heterojunction and the accelerated mass transfer effect of oxygen vacancies. LCSM tests visually and powerfully demonstrated the photocatalytic antibacterial ability of concrete/TiO_2/Ag materials. In conclusion, this study has developed a concrete-based environmental functional material with photocatalytic self-cleaning properties, with broad application prospects. In the long run, this approach also provides valuable insights for the practical design of photocatalytic materials.

Acknowledgements

Financial support from Scientific and technological development plan project in Jilin Province of China (No.20220508146RC) and (20210203141SF) are acknowledged. In addition, Dr Ziming Shang of the Research Center for Eco-Environmental Sciences, Chinese Academy of Sciences, contributed to this study.

References

Qiao, X. J., Liao, K. H., & Randrup, T. B. (2020). Sustainable stormwater management: A qualitative case study of the Sponge Cities initiative in China. *Sustainable Cities and Society*, **53**, 101963.

Qi, B., Gao, S., & Xu, P. (2023). The application of rubber aggregate-combined permeable concrete mixture in sponge city construction. *Coatings*, **13**(1), 87.

Jiang, W., & Gan, J. (2016). Conversion of pesticides to biologically active products on urban hard surfaces. *Science of The Total Environment*, **556**, 63-69.

Kiledal, E. A., Keffer, J. L., & Maresca, J. A. (2021). Bacterial communities in concrete reflect its composite nature and change with weathering. *Msystems*, **6**(3),

e01153-20.

Nath, R. K., Zain, M. F. M., & Jamil, M. (2016). An environment-friendly solution for indoor air purification by using renewable photocatalysts in concrete: A review. *Renewable and Sustainable Energy Reviews*, **62**, 1184-1194.

Topçu, I. B., Akkan, E., Uygunoğlu, T., & Çalişkan, K. (2020). Self-cleaning concretes: an overview. J. *Cem. Based Compos*, **2**, 6-12.

Rammohan, G., & N Nadagouda, M. (2013). Green photocatalysis for degradation of organic contaminants: a review. *Current Organic Chemistry*, **17**(20), 2338-2348.

Guo, Z., Huang, C., & Chen, Y. (2020). Experimental study on photocatalytic degradation efficiency of mixed crystal nano-TiO_2 concrete. *Nanotechnology Review*s, **9**(1), 219-229.

Petronella, F., Pagliarulo, A., Truppi, A., Lettieri, M., Masieri, M., Calia, A., ... & Comparelli, R. (2018). TiO_2 nanocrystal based coatings for the protection of architectural stone: the effect of solvents in the spray-coating application for a self-cleaning surfaces. *Coatings*, **8**(10), 356.

Abbas, M., Mehran, M. T., Moon, M. W., Byun, J. Y., & Kim, S. H. (2020). Wettability control of modified stainless steel surfaces for oxide catalyst carrier slurry coating. *Journal of Industrial and Engineering Chemistry*, **91**, 330-339.

Zhang, X., Lin, G., Ma, S., Liu, M., Jiang, W., & Wu, C. (2022). Efficiency and durability of carbon dots grafted TiO_2-based coatings applied on concrete under peeling and washing trials. *Diamond and Related Materials*, **129**, 109333.

Munafo, P., Goffredo, G. B., & Quagliarini, E. (2015). TiO_2-based nanocoatings for preserving architectural stone surfaces: An overview. *Construction and Building Materials*, **84**, 201-218.

Liu, N., Ming, J., Sharma, A., Sun, X., Kawazoe, N., Chen, G., & Yang, Y. (2021). Sustainable photocatalytic disinfection of four representative pathogenic bacteria isolated from real water environment by immobilized TiO_2-based composite and its mechanism. *Chemical Engineering Journal*, **426**, 131217.

Zhao, L., Chen, R., Pang, L. X., Zhang, W., & Tan, X. (2019). Study on Photo-catalytic Efficiency and Durability of Nano-TiO_2 in Permeable Concrete Pavement Structure. In IOP Conference Series: *Earth and Environmental Science*, **371**, 4, 042011.

Shang, Z., An, X., Liu, H., Hu, C., & Qu, J. (2021). Silvered TiO_2 for facet-dependent photocatalytic denitrification. *ACS Applied Nano Materials*, **4**(12), 13534-13542.

Abetua, A. G., & Kebedeb, A. B. (2021). Crushed concrete as adsorptive material for removal of phosphate ions from aqueous solutions. *Water Cons Manage*, **2**, 40-46.

Gaylarde, C. C., & Morton, L. G. (1999). Deteriogenic biofilms on buildings and their control: a review. *Biofouling*, **14**(1), 59-74.

Gladis, F., Eggert, A., Karsten, U., & Schumann, R. (2010). Prevention of biofilm growth on man-made surfaces: evaluation of antialgal activity of two biocides and photocatalytic nanoparticles. *Biofouling*, **26**(1), 89-101.

Cho, M., Chung, H., Choi, W., & Yoon, J. (2004). Linear correlation between inactivation of E. coli and OH radical concentration in TiO_2 photocatalytic

disinfection. *Water research*, **38**(4), 1069-1077.

Huang, Y., Li, K., Zhou, J., Guan, J., Zhu, F., Wang, K., & Li, N. (2022). Nitrogen-stabilized oxygen vacancies in TiO_2 for site-selective loading of Pt and CoOx cocatalysts toward enhanced photoreduction of CO2 to CH4. *Chemical Engineering Journal*, **439**, 135744.

Khiem, T. C., Huy, N. N., Kwon, E., Lee, J., Da Oh, W., Duan, X., & Lin, K. Y. A. (2024). Electron transfer-mediated enhancement of superoxide radical generation in fenton-like process: Key role of oxygen vacancy-regulated local electron density of cobalt sites. *Applied Catalysis B: Environmental*, **343**, 123490.